www.trjfas.org
ISSN 1303-2712
Turkish Journal of Fisheries and Aquatic Sciences 17: 257-268 (2017) DOI: 10.4194/1303-2712-v17_2_04

RESEARCH PAPER

Structural Analysis of Float Collar for Metal Fish Cage in Waves

Tiao-Jian Xu[1,2], Hui-Min Hou[1], Guo-Hai Dong[1], Yun-Peng Zhao[1], Wei-Jun Guo[3]

[1] State Key Laboratory of Coastal and Offshore Engineering, Dalian University of Technology, Dalian 116024, China.
[2] School of Naval Architecture and Ocean Engineering, Dalian University of Technology, Dalian 116024, China.
[3] Environmental Science and Technology College, Dalian Maritime University, Dalian 116026, China.

* Corresponding Author: Tel.: +86.411 84708514; Fax: +86.411 84708526;
E-mail: tjxu@dlut.edu.cn

Received 28 October 2015
Accepted 07 September 2016

Abstract

Float collar is an important component for the fish cage systems which are applied by the aquaculture industry. The integrity and reliability of the float collar are detrimental in order to avoid the critical failure which may lead to major loss and severe consequences. A finite element model for the structural analysis of the float collar for the metal fish cage in waves is developed and validated by comparing with the experimental data. The numerical simulation is performed to conduct the parametrical study of float collar and to analyze the deformation and the stress of a metal fish cage in waves. The results indicate that the numerical model can accurately predict the deformation of float collar and the tension force on mooring line. When the central angle of the arc between two neighboring clamps is larger than 15°, the influence of the amount of clamps on the deformation of float collar is decreased significantly. For the metal fish cage structure, the upper part of the nets for the metal fish cage experiences the largest deformation, and thus the diameter of the net twine at the upper part of the metal fish cage should be increased to avoid the structural failure.

Keywords: Finite element analysis, Deformation, Metal net cage, Numerical simulation.

Introduction

Fish farms are recently forced to move into the offshore area, and this makes a challenge for the design of fish cage structure, especially for the structural analysis of float collar for the gravity cage. The float collar for gravity cage is the primary component to withstand the wave force, and its design plays an important role for the safety of the fish cage structure (see Figure 1). Therefore, it is necessary to analyze the deformation and the stress of the float collar, which is the basis for the design and safety assessment of the fish cage system.

To our knowledge, several researches were conducted to analyze the dynamic response of fish cage in the open sea. Some studies including numerical simulation and physical model test were focused on the hydrodynamic behavior of net cages in waves and currents. Ormberg (1991) extended the existing FEM program RIFLEX (SINTEF, 1987) to perform dynamic, nonlinear analysis of floating fish farms in regular waves. Tsukrov *et al*. 2003 proposed a numerical model to analyze the hydrodynamic response of net panels to environmental loading with the concept of consistent finite element. Lader and Fredheim 2006 investigated dynamic properties of a flexible net sheet exposed to waves and current by numerical simulation, in which the net was modeled by dividing it into super elements. Kristiansen and Faltinsen 2012 proposed a screen type of force model for the viscous hydrodynamic load on nets, in which the net is divided into a number of flat net panels, or screens. Li *et al*. 2013 investigated the nonlinear hydroelastic response of a deep-water gravity aquaculture fish cage in irregular waves. Fu *et al*. 2013 investigated the hydrodynamic characteristics of a floating cylinder for fish cage by the force oscillation experiments in towing tank.

In addition, the mechanical performance of net material used in the fish cage structure was also analyzed. Sala *et al*. 2004 investigated experimentally the differences in breaking load and elongation of knotless netting before and after use. Moe *et al*. 2007 established a new method to investigate the tensile stiffness properties of knotless netting material. Moe *et al*. 2008 investigated the temporary-creep properties, recovery of strain post creep and post-creep tensile properties of a selection of Raschel knitted netting materials.

Furthermore, Suhey *et al*. 2005 presented a numerical simulation of an inflatable open-ocean-aquaculture cage using nonlinear finite element

Figure 1. Common failure mode of the float collar for fish cage.

analysis of membrane structures, and the finite element model is validated using a modified beam theory for the inflatable structure by comparing the maximum deflection and stress. Fredriksson *et al*. 2007 developed a finite-element modeling technique to determine the structural capabilities of net pens, in which the critical loading conditions are predicted. Dong *et al*. 2010 proposed an analytical method to investigate the elastic deformations of a circular ring subjected to water waves, based on the Euler's laws and the curved beam theory. Xu *et al*. 2014 analyzed the fatigue damage of mooring line for net cage using the rainflow counting method and the spectrum analysis method. Kim *et al*. 2014 analyzed the flow field characteristics within the abalone containment structure with computational fluid dynamic software, in addition, the structural analysis of the deployment and recovery operation was also investigated.

Recently, the metal net cage has received much attention from the researcher due to such advantages as the protection from predators, the better cage volume retention, and the good resistance to bio-fouling. Tsukrov *et al*. 2011 conducted a series of experiments to analyze the drag forces on copper alloy net panels, and proposed the empirical values for normal drag coefficients for various types of copper netting. Cha *et al*. 2013 analyzed the drag and lift coefficients of copper alloys and fabric nets, and observed the flow through the fish net using particle image velocimetry (PIV). However, the existing research has never concerned with the structural analysis of the fish cage with metal nets. The research on the deformation and the stress of the float collar with metal fish net under the action of waves is very limited, and the bending stiffness of fish net is usually neglected in the previous numerical model developed for fish cage. Therefore, it is necessary to develop a numerical model for analyzing the structural performance of the float collar with metal fish net in waves. Thus, the finite element technique is used to build the numerical model for the structural analysis of float collar with metal fish nets in waves here, in which the dynamic load test is performed. In this study, the numerical simulation for the structural analysis of the float collar with metal fish nets was conducted, and the parametrical study of the float collar was also performed.

The paper is organized as follows. Section 2 presents a description of the numerical method for the structural analysis of the float collar with metal nets in waves. Section 3 describes a physical model test of a float collar and mooring system and presents the comparison results between the numerical simulation and the physical model tests. In Section 4, the parametrical study of float collar in waves is performed and the structural analysis of a metal fish cage is also conducted. Finally, Section 5 summarizes some conclusions.

Method

The finite element model of the float collar with metal nets in waves was described here. The load-deformation model for the structural analysis of float collar in waves was developed in the commercially available software ANSYS, and the pipe element is applied to simulate the float collar and the link element is used to model the mooring lines

Governing Equation

Transient dynamic analysis is a technique used to determine the dynamic response of a structure under the action of any general time-dependent loads. This analysis can be used to determine the time-varying displacements, strains, stresses, and forces in a structure as it responds to any combination of static, transient and harmonic loads. The basic equation of motion solved by a transient dynamic analysis is as follows,

$$[M]\{\ddot{R}\}+[C]\{\dot{R}\}+[K]\{R\}=\{F(t)\}+\{P(t)\} \quad (1)$$

where R is the nodal displacement vector, $\dot{R}$ is the nodal velocity vector, $\ddot{R}$ is the nodal acceleration vector, M is the mass matrix, C is the damping matrix, K is the stiffness matrix, $F(t)$ is the equivalent nodal

force vector due to relative fluid motion, the wave and current loads, $P(t)$ is the equivalent nodal force due to gravity and buoyancy forces. The Newmark time integration method is applied to solve these motions at discrete time points.

For the finite element model of the float collar with metal nets, the pipe element is applied to simulate the floating pipe and the link element is used to model the mooring line. The pipe element applied here is a uniaxial element with tension-compression, torsion, and bending capabilities, and with the member forces simulating the ocean waves and current. The pipe element has six degrees of freedom at each node: translations in the nodal *x*, *y*, and *z* directions and rotations around the nodal *x*, *y*, and *z* axes. The element loads include the hydrodynamic and buoyant effects of the water, and the element mass includes the added mass of water and the pipe internals. In addition, the pipe element was simplified to simulate the cage net structure, in which the inner diameter of the pipe element is set to be zero for simulating the nets and the bending stiffness of the nets is also considered in the numerical model. The geometry, node locations, and the coordinate system for this element are shown in Figure 2.

Environmental Loading

The hydrodynamic load acting on the floating pipe is calculated from a generalized Morison's equation. To simplify the numerical model, each element is treated as a small body since the element size is relatively small compared with the characteristic wavelength. This means that the scattering effect between the structural element and the flow field can be neglected. Thus, it is appropriate to apply the modified Morison equation including the relative motion between the structural element and the surrounding fluid, as follows:

$$F = \frac{1}{2} C_D \rho A \left| u - \dot{R} \right| \cdot (u - \dot{R}) + \rho V_0 a + C_m \rho V_0 (a - \ddot{R}) \qquad (2)$$

where u and $\dot{R}$ are the velocity vectors for the water particles and the structural elements, respectively; a and $\ddot{R}$ are the acceleration vectors for the water particles and the structural elements, respectively; ρ is the density of water; V_0 is the water displaced volume of a structural element; A is the effective projected area of a structural element, and C_D and C_m are the drag and added mass coefficients, respectively. The hydrodynamic coefficients of float collar are taken as constants: the drag coefficients are chosen as C_D=0.4; and the added mass coefficients are chosen as C_m=0.2.

Description of Wave Field

Based on linear wave theory, the velocity potential of the wave is given by

$$\phi = -A \frac{g}{2\pi f} \frac{\cosh k(d+z)}{\cosh kd} \sin(kx - 2\pi ft) \qquad (3)$$

Surface elevation,

$$\eta = A\cos(kx - 2\pi ft) \qquad (4)$$

and dispersion relation,

$$(2\pi f)^2 = gk \tanh(kd) \qquad (5)$$

where A is the wave amplitude, g is the gravitational acceleration, f is the wave frequency, k is the wave number (equal to $2\pi/L$), L is the wave length, d is the water depth, z is the vertical distance (positive upward) from mean-water level.

Metal Fish Cage Model

The metal fish cage has received much attention due to its strong anti-wave and anti-current performance. A typical two-ring metal fish cage in Figure 3 is usually composed of floating pipe, handrail, stanchion and clamps. The clamps between the rings keep them at correct distance, and the inner ring (diameter = 15.92 m) is connected with the outer ring (diameter = 16.92 m) by a series of clamps. The center to center distance between the rings is 0.5 m.

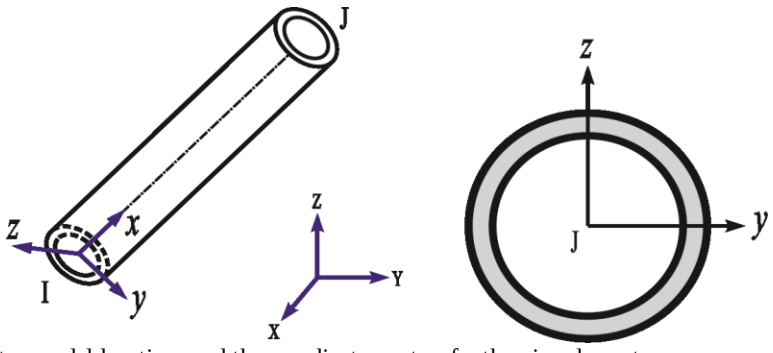

Figure 2. The geometry, nodal locations and the coordinate system for the pipe element.

The two rings are made of pipes with identical cross-section properties: diameter: 25 cm, wall thickness: 1.3 cm, modulus of elasticity: E = 667 Mpa, density: 953 kg/m^3. The clamps are modeled assuming a pipe of HDPE with circular cross-section with radius of 25 cm. The stanchion with height of 1 m is used to link the handrail and the inner ring. There are 3648 nodes and 3696 pipe elements in the finite element model of float collar, and the maximum mesh size of the pipe element is 2 cm.

There are 120 meshes in the circumferential direction and 15 in the depth direction for the fish net. The net is knotless, with a mesh size of 59 mm and a twine thickness of 2.4 mm. When mounted as diamond meshes, the net forms an open vertical cylinder with a diameter of 15.92 m and a height of 6.258 m. The net is attached to the float collar, and the mass density of the metal fish net is 7.85×10^3 kg/m^3. The metal fish cage is anchored to the sea floor by the four mooring lines. The water depth is 20 m, and the coordinates of the four anchor points are (50, 50, -20), (-50, 50, -20), (-50, -50, -20), (50, -50, -20), respectively.

Physical Model Test

A series of physical model tests were conducted to validate the numerical model for the structural analysis of float collar for fish cage in waves. The model test includes two parts: the structural analysis of the circular ring and the hydrodynamic response of float collar in waves.

Circular Ring Experiments

To validate the finite element model for the structural analysis the float collar in waves, a set of experiments were conducted using circular rings of HDPE pipe. Tests were first conducted in the laboratory, and then the numerical simulations were performed using the FEM technique.

The 84.6 cm diameter circular ring of HDPE pipe (pipe diameter = 15.32 mm, pipe thickness = 1.33 mm) is tested in the laboratory experiment, the ring was fixed at two locations on one side spaced approximately 59.8 cm (along the arc). On the other side, a single rope with an inline load cell was attached to the ring. A photograph of the setup is shown in Fig. 4a. The deformation of the circular ring under the action of the concentrated load is shown in Figure 4. The next step was to perform numerical simulations of the circular ring laboratory tests and compare the results. The finite element model of the circular ring was constructed using the geometric properties of the pipe from the circular ring laboratory tests. The deformation of the circular ring from the numerical simulation is also shown in Fig. 3. The results indicate that the shapes of circular ring from the numerical simulation are similar with those from the physical model test.

The quantitative comparison of the diametric deflection between the numerical simulation and the

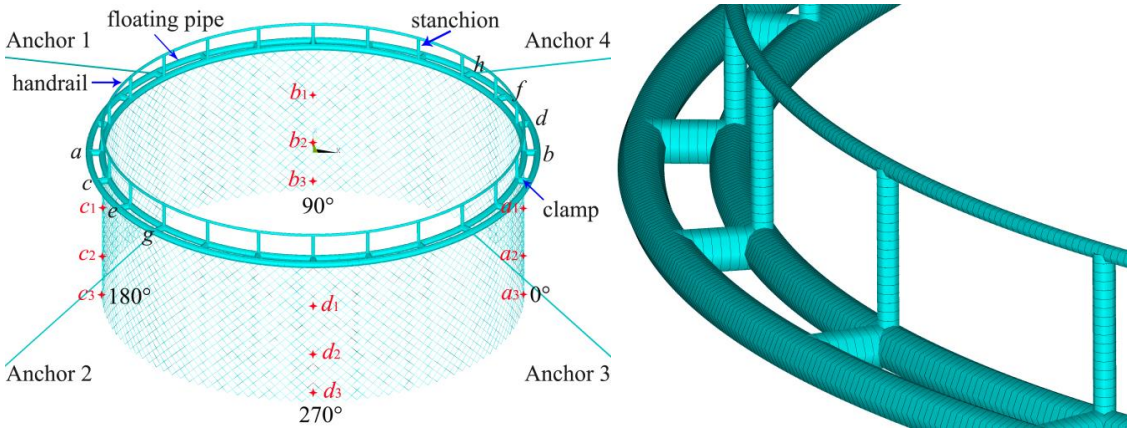

Figure 3. The finite element model of the fish cage with metal nets.

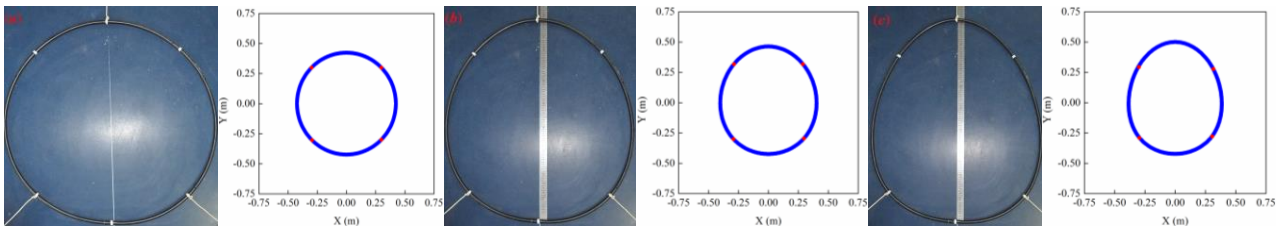

Figure 4. The circular ring under the action of point loads (a) initial shape, (b) F=0.5 kg, (c) F=1 kg.

physical model test is also presented here. As shown in Figure 5, the measured tension is plotted as a function of diametric deflection of the circular ring. It indicates that the finite element model is appropriate to investigate the deformation of circular rings under external loads.

Float Collar in Waves

To validate the finite element model for the float collar in waves, the numerical simulation for the hydrodynamic response of float collar in waves was performed and compared with the physical model tests (Figure 6). The tests were conducted in the wave-current basin at the State Key Laboratory of Coastal and Offshore Engineering of the Dalian University of Technology, China. The wave-current basin is 69 m long, 2 m wide and 1.8 m high. The SG800 wave probe produced by the China Institute of Water Resources and Hydropower Research is applied to measure wave height and period, with measuring range of 0-35 cm and relative error of 0.5%. The DJ800 with the measuring range is 0-10 N is adopted to measure the tension force on mooring line.

The float collar model should meet the geometric similarity, kinematic similarity and dynamic similarity. However, it is difficult to completely meet the similarity law. Because the float collar is usually at the surface of water, the double floating pipes are the main components to withstand the hydrodynamic force. Therefore, the float collar is simplified into double concentric pipes in the physical model test. The float collar model is designed to satisfy the geometric similarity and gravity similarity. The detailed parameters of the float collar are given in Table 1 and Table 2.

Measurements of the mooring line forces were obtained using a submersible, ring-type load cell, which is attached to the bottom of the anchor lines. An optical measurement system was developed to determine the float collar motions. Two diodes were fixed on the float collar for motion analysis, as shown in Fig. 6. A charge coupled device (CCD) camera recorded the movements of diodes. The camera captures a series of images and transfers each frame to the computer and temporary storage. Later, specially written software is used to search the position of diodes, which is used to calculate the float collar horizontal and vertical movements as functions of

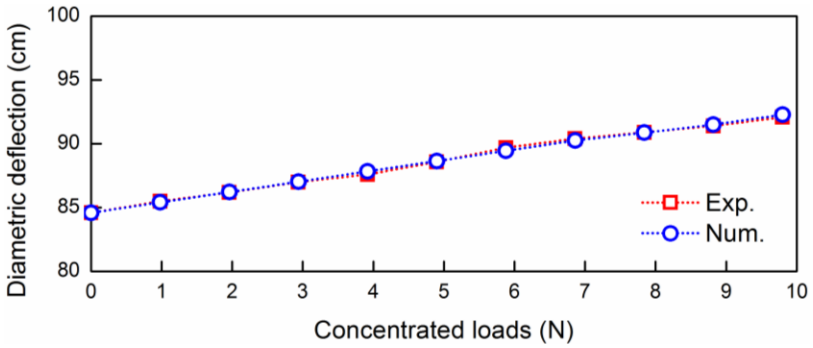

Figure 5. The diametric deflection of a circular ring under the action of point loads.

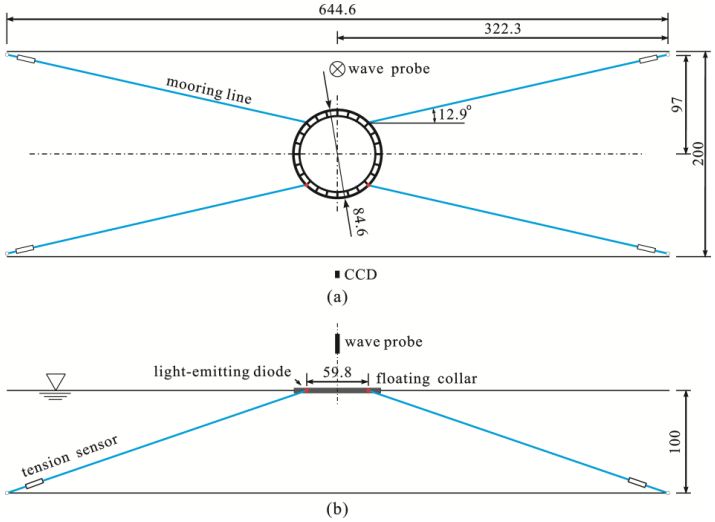

Figure 6. Schematic of the physical model of float collar for net cage system, (a) vertical view and (b) front view.

time. The regular waves propagated along the positive *x*-direction. The details of regular wave conditions are presented in Table 3.

The calculated and experimental results were quantitatively compared to validate the numerical model. The mooring line tension force and the float

Table 1. Geometry and material parameters of float collar

Component	Parameter	value
Outer circle	General diameter (m)	0.846
	Pipe inner diameter (mm)	15.32
	Pipe outer diameter (mm)	12.66
	Density (g/cm^3)	0.953
	Material	HDPE
Inner circle	General diameter (m)	0.796
	Pipe inner diameter (mm)	15.32
	Pipe outer diameter (mm)	12.66
	Density (g/cm^3)	0.953
	Material	HDPE

Table 2 Mechanical parameters of HDPE used in the float collar

Parameter	Value
Elastic modulus	667M Pa
Yield limit	24.1MPa
Poisson ratio	0.41
Density	953 kg/m^3

Table 3 Wave parameters for numerical simulation and physical model test

No.	1	2	3	4	5	6	7	8	9	10	11	12
Wave period *T* (s)	1.2	1.4	1.6	1.4	1.6	1.8	1.4	1.6	1.8	1.6	1.8	2.0
Wave height *H* (cm)	20	20	20	25	25	25	29	29	29	34	34	34

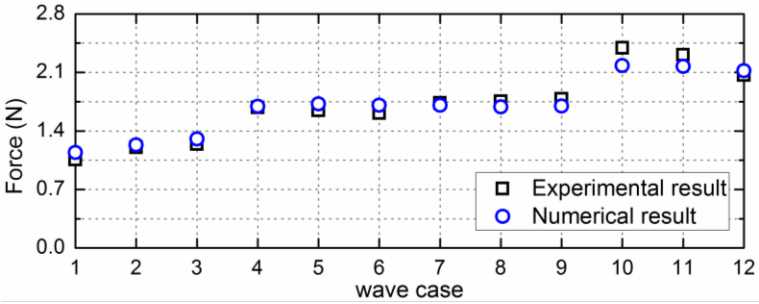

Figure 7. The tension force on anchor line from the numerical simulation and physical model test.

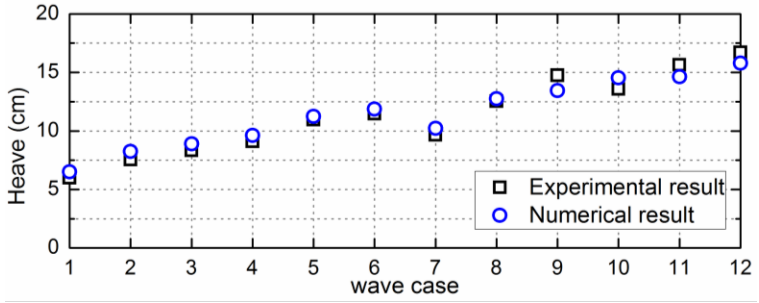

Figure 8. The heave motion of float collar from the numerical simulation and physical model test.

collar motion are selected for comparison. For the mooring line tension force, the designer of the fish cage and mooring system is mainly focused on the maximum value of the mooring line tension force. Figure 7 shows the comparisons of the maximum mooring line tension force obtained from the calculated results and experimental data. Figures 8 and 9 compare the maximum vertical and horizontal displacements of the float collar obtained from the calculated results and experimental data, respectively.

The relative error is given by $\varepsilon=(V_s-V_m)/V_m$, where V_s and V_m are the maximum mooring line tension forces and the motion responses of float collar obtained from the numerical simulation and the physical model test, respectively. For the maximum mooring line tension force, the maximum relative error is 8.7% and the mean value of the relative error is 4.6%. For the motion response of the float collar, the maximum errors of the vertical and horizontal displacements of the float collar are 9.2% and 10.6%, respectively. The mean relative errors of the vertical and horizontal displacements of the float collar are 5.9% and 6.2%, respectively.

The calculated results of the tension forces on mooring line and the motions of float collar correspond well with the experimental data, with the relative errors of approximately 11%. Based on the above analysis, the numerical model presented here can be used in the structural analysis of the float collar under the action of waves.

Results and Discussion

The numerical simulation for the structural analysis of the float collar in waves is performed to analyze the deformation and the stress of the float collar. The parametrical study of the float collar is conducted, and then the structural analysis of a metal fish cage is also performed. A 2 m wave with period of 6 s is applied here.

Effect of the Amount of Connectors

The amount of connectors including the clamp and the stanchion will affect the deformation of float collar, it is necessary to choose an appropriate amount of connectors. The central angle θ of an arc between the neighboring connectors for different amount of connectors (18, 24, 30 and 36) is equal to 20°, 15°, 12° and 10°, respectively.

The deformation rate $C_{ab}=(l_{ab}-D)/D$ is applied to represent the deformation of float collar, where D is the diameter of float collar, l_{ab} is the maximum value of the distance between the points a and b, and the initial value of l_{ab} is equal to the diameter of float collar. The points a, b, c, d, e, f, g and h are marked in Fig. 3 for clarity of the description. Similarly, the deformation rate C_{cd}, C_{ef} and C_{gh} can also be obtained.

The deformation C_{ab} of float collar with different amount of connectors is shown in Figure 10. When the amount of connectors is 18, 24, 30 and 36, the deformation rate C_{ab} of float collar is 1.8%, 1.32%, 1.3%, and 1.27%, respectively. It indicates that with the increase in the amount of connectors, the deformation of float collar is decreased significantly. When the central angel θ is larger than 15° (i.e. the amount of connectors is 24), the influence of the amount of connectors on the deformation of the float

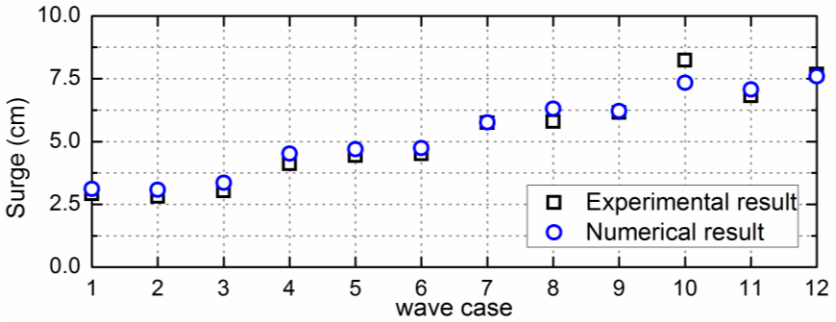

Figure 9. The surge motion of float collar from the numerical simulation and physical model test.

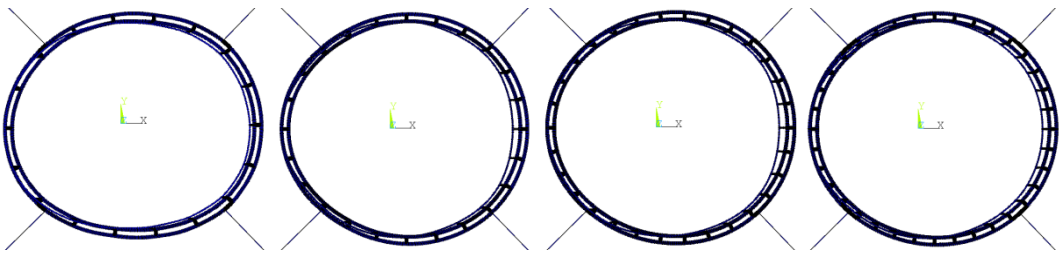

Figure 10. The largest deformation of the float collar in the x axis.

collar is becoming smaller.

The maximum stress on the float collar is also calculated and shown in Figure 11. The results indicate that the maximum stresses on the inner ring and the outer ring are generally decreased with the increase in the amount of connectors. As the increase in the amount of connectors, the deformation of float collar is decreased, and thus it is reasonable that the maximum stress on the float collar is also decreased with the increasing amount of connectors.

Effect of the Bending Rigidity of Connectors

In order to reduce the deformation of float collar in waves, the float collar must have sufficient bending stiffness. The relative rigidity between the connector and the floating pipe will affect the deformation mode of float collar, and thus different rigidities of connectorare considered, as shown in Table 4.

The deformations of float collar with different rigidities of connectors are shown in Figure 12. The deformation of float collar in waves includes the in-plane deformation and the out-of-plane deformation. The results indicate that the relative rigidity between the connectors and the floating pipes has significant influence on the in-plane deformation; however, its influence on the out-of-plane deformation is relatively small. The deformation of float collar is increased with the decrease in the bending stiffness of connectors. The out-of-plane deformation is largest as the wave crests or the wave troughs pass through the center of float collar, in addition, the element of floating pipe connected with the mooring line experiences the largest bending deformation.

The deformation of handrail is also increased with the decrease in the bending stiffness of connectors as shown in the fourth row of Fig. 12. It is reasonable because the bending stiffness of the float collar is decreased as the bending stiffness of connectors is decreased, and thus the deformation of float collar is increased. The handrail for the float collar is generally located above the water surface, and thus the double floating pipes are the main component to withstand the hydrodynamic force. When a larger deformation of float collar occurs, more of the hydrodynamic loads acting on the double floating pipes can be transferred into the handrail.

Effect of the Tensile Stiffness of Mooring Line

The float collar is anchored to the sea floor by mooring line. Different stiffness values of mooring line are considered here, and the tensile stiffness ($K=EA/l$) of mooring line is set as 1.1×10^2, 1.1×10^3, 1.1×10^4, 1.1×10^5, 1.1×10^6 N/m, respectively. The maximum tension force on the mooring line and the diametrical deformation of float collar for different tensile stiffness values of mooring line are calculated and compared, as shown in Figure 13. The results indicate that the maximum tension force on mooring line is increased significantly with the increase in the tensile stiffness of mooring line. The deformation rate of float collar is also increased with the increasing tensile stiffness of mooring line. It means that as long as the breaking strength of mooring line is enough, it is better to select a lower mooring line tensile stiffness

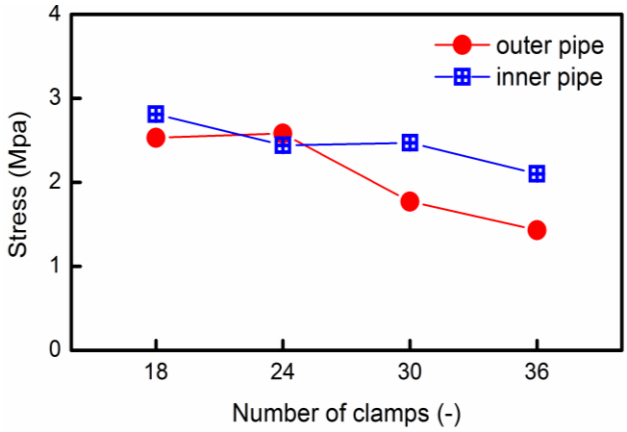

Figure 11. Maximum stress on the float collar with different amount of connectors.

Table 4 Bending stiffness of the connector and the floating pipe

No.	EI_{cl} (N·m^2)	EI_{cl}/EI_{pipe}	EI_{st}	EI_{st}/EI_{pipe}
1	9.0×10^3	0.1	8.0×10^2	8.8×10^{-3}
2	9.0×10^4	1	8.0×10^3	8.8×10^{-2}
3	9.0×10^5	10	8.0×10^4	8.8×10^{-1}
4	9.0×10^6	100	8.0×10^5	8.8

cl represents clamp, *st* represents stanchion.

to reduce the structural response of float collar in waves.

Different Wave Incident Direction

Note that the waves propagated along various directions in the open sea, and it will affect the structural response of float collar structure. Thus, four different wave directions (0°, 15°, 30° and 45°) are considered in view of the symmetrical characteristics of the fish cage and mooring system. The deformation rates C_{ab}, C_{cd}, C_{ef} and C_{gh} of the float collar (see Fig. 3) are calculated for different wave incident

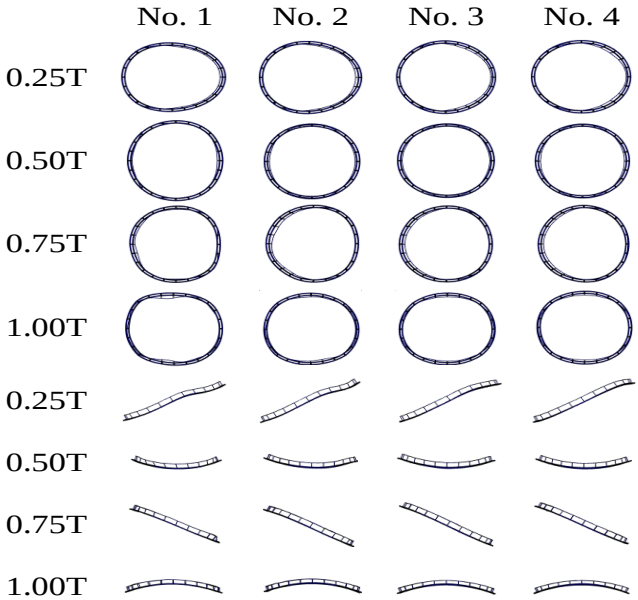

Figure 12. The deformation of float collar with different rigidity of connectors.

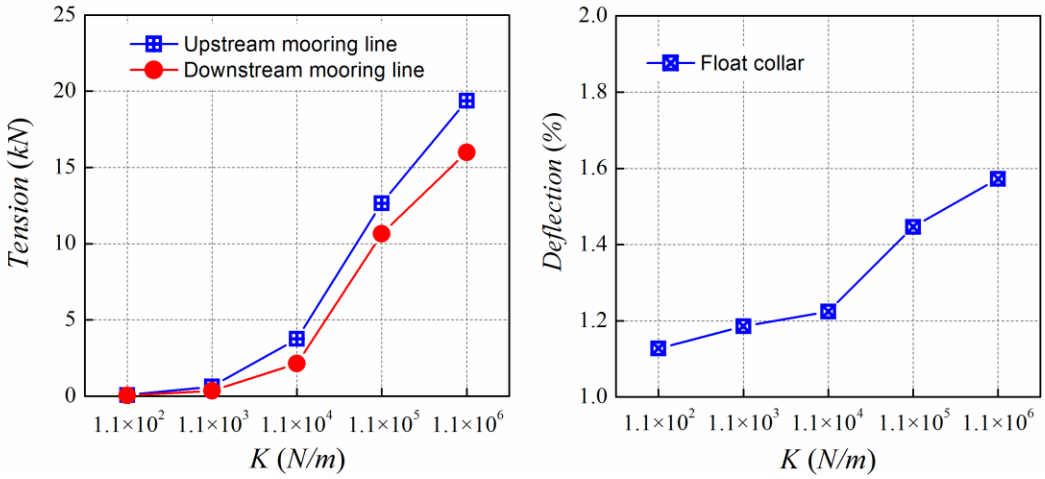

Figure 13 The maximum tension force on mooring line and the deflection of float collar with different stiffness of mooring line.

Table 5 The deformation rate of float collar and the maximum tension force on mooring line for different wave incident directions

Direction	0°	15°	30°	45°
C_{ab} (%)	1.22	1.11	1.02	0.60
C_{cd} (%)	1.21	1.46	1.20	0.88
C_{ef} (%)	1.03	1.43	1.46	1.39
C_{gh} (%)	0.72	1.07	1.34	1.55
T (kN)	3.75	4.51	4.44	4.78

directions, as shown in Table 5. The results indicate that the largest deformation of float collar is always occurred in the wave incident direction. When the wave incident direction is along the mooring lines, the deformation of float collar is largest. The maximum tension forces on mooring line are also presented in Table 5. When the wave incident angle is 45°, the maximum tension force on mooring line is largest.

Fish Cage with Metal Nets

Figure 14 shows the maximum stress on the net for the metal fish cage at different points marked with star shape in Fig. 3. The results indicate that when the depth is larger than 4.2 m, the variation of the maximum stress on the net for the metal fish cage is small, and the maximum stress on the upper part of the net is obviously larger than that for the lower part of the net. Thus, only the twine diameter at the upper part of the nets for the metal fish cage should be increased.

The deformations of the nets for the metal fish cage in waves at four representative moments are calculated and shown in Figure 15. The results indicate that the upper part of the net for the metal fish cage experiences the largest deformation, which is consistent with the stress distribution on the cage net. The deformation of the lower part of the net for the metal fish cage is small, which is obviously different from that for the flexible net cage (Xu *et al*. 2013). In addition, when the wave crest and the wave trough pass through the center of the fish cage, the largest out-of-plane deformation of the float collar occurs, which significantly affect the deformation of the cage net.

The bending stiffness of float collar will affect the out-of-plane deformation of float collar in waves. To know how the deformation of float collar will influence the deformation and the stress of the fish net for the metal fish cage, and thus two kinds of bending stiffness of the float collar (E_1=667 Mpa, E_2=6670 Mpa) are considered here. Figure 16 presents the maximum stress on the fish net at points a_1, b_1, c_1 and d_1 (see Fig. 3) for two kinds of bending stiffness of the float collar, respectively. The results indicate that the bending stiffness of the float collar significantly affect the maximum stress on the fish net at point c_1, however, the influence of the bending stiffness of float collar on the stress on the fish net at points b_1 and d_1 is relatively small. Based on the above analysis, the fish farmer should strengthen to detect the deformation and the stress of the upper part of the metal fish cage.

Conclusions

Transient finite element analysis of a metal fish cage and mooring system in waves is performed to analyze the deformation and the stress of the metal fish cage. A series of physical model test is conducted

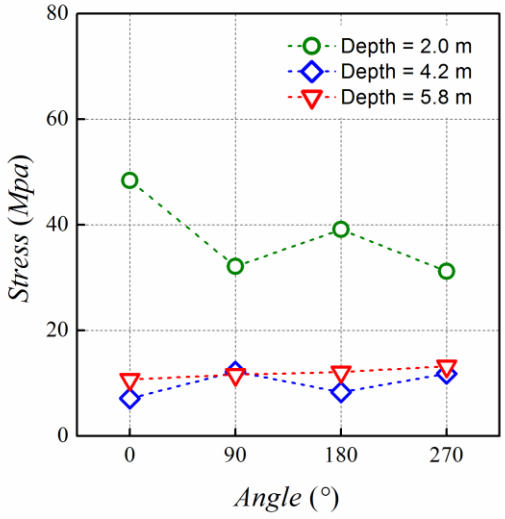

Figure 14. The distribution of the maximum stress on the cage net at different position.

Figure 15. The deformation of the nets for the metal fish cage at the representative moments.

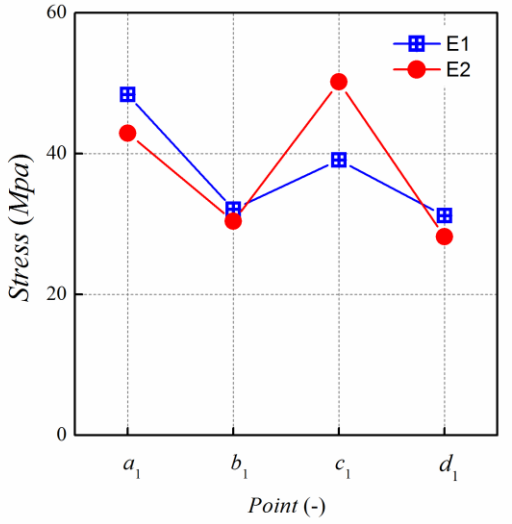

Figure 16. Stress on the fish net for different bending stiffness of float collar.

to validate the numerical model. The results indicate that the numerical model is suitable for analyzing the deformation of float collar and the tension force on mooring line. The parametrical study of float collar shows that the effect of the amount of connectors on the deformation of float collar is becoming smaller when the central angel θ of the arc between two neighboring connectors is larger than 15°. The out-of-plane deformation of the float collar is most serious as the wave crests and the wave troughs pass through the center of float collar. The largest deformation of float collar is always occurred in the wave incident direction. The maximum stress on the upper part of the net for the metal fish cage is significantly larger than that for the lower part of the net, and the deformation of the metal fish-cage is primarily occurred at the upper part of the net. The fish farmer should strengthen to detect the stress and deformation of the upper part of the net for the metal fish cage.

Acknowledgements

This work was financially supported by the National Natural Science Foundation (NSFC) Projects No. 51409037, 51239002, 51579037, and 51221961, China Postdoctoral Science Foundation (No.2014M560211 and No.2015T80254), the Fundamental Research Funds for the Central Universities No. DUT16RC(4)25, and Cultivation plan for young agriculture science and technology innovation talents of Liaoning province (No.2014008).

References

Cha, B.J., Kim, H.Y., Bae, J.H., Yang, Y.S., Kim, D.H., 2013. Analysis of the hydrodynamic characteristics of chain-link woven copper alloy nets for fish cages. Aquacultural Engineering 56, 79-85. DOI: 10.1016/j.aquaeng.2013.05.002

Dong, G.H., Hao, S.H., Zhao, Y.P., Zong, Z., Gui, F.K., 2010. Elastic responses of a flotation ring in water waves. Journal of Fluids and Structures 26(1), 176-192. DOI: 10.1016/j.jfluidstructs.2009.09.001

Fredriksson, D.W., Decew, J.C., Tsukrov, I., 2007. Development of structural modeling techniques for evaluating HDPE plastic net pens used in marine aquaculture. Ocean Engineering 34, 2124-2137. DOI: 10.1016/j.oceaneng.2007.04.007

Fu, S.X., Xu, Y.W., Hu, K., Zhang, Y., 2013. Experimental investigation on hydrodynamic of floating cylinder in oscillatory and steady flows by forced oscillation test. Marine Structures 34, 41-55. doi:10.1016/j.marstruc.2013.08.005

Kim, T., Lee, J., Fredriksson, D.W., DeCew, J., Drach, A., 2014. Engineering analysis of a submersible abalone aquaculture cage system for deployment in exposed marine environments. Aquacultural Engineering 63, 72-88. DOI: 10.1016/j.aquaeng.2014.10.006

Kristiansen, T., Faltinsen, O.M., 2012. Modelling of current loads on aquaculture net cages. Journal of Fluids and Structures 34, 218-235. DOI: 10.1016/j.jfluidstructs.2012.04.001

Lader, P.F., Fredheim, A., 2006. Dynamic properties of a flexible net sheet in waves and current-A numerical approach. Aquacultural Engineering 35(3), 228-238. DOI: 10.1016/j.aquaeng.2006.02.002

Li, L., Fu, S.X., Xu, Y.W., 2013. Nonlinear hydroelastic analysis of an aquaculture fish cage in irregular waves. Marine Structures 34, 56-73. DOI: 10.1016/j.marstruc.2013.08.002

Moe, H., Hopperstad, O.S., Olsen, A., Jensen, Fredheim, A., 2008. Temporary creep and post creep properties of aquaculture netting materials. Ocean Engineering 36(12-13), 992-1002. DOI: 10.1016/j.oceaneng.2009.05.009

Moe, H., Olsen, A., Hopperstad, O.S., Jensen, Ø., Fredheim, A., 2007. Tensile properties for netting materials used in aquaculture net cages. Aquacultural Engineering 37(3), 252-265. DOI: 10.1016/j.aquaeng.2007.08.001

Ormberg, H. (1991). Non-linear response analysis of floating fish farm systems. PhD thesis, Division of

Marine Structures, Norwegian Institute of Technology, University of Trondheim.

Sala, A., Lucchetti, A., Buglioni, G., 2004. The change in physical properties of some nylon (PA) netting samples before and after use. Fisheries Reserach 69, 181-188. DOI: 10.1016/j.fishres.2004.05.005

Suhey, J.D., Kim, N.H., Niezrecki, C., 2005. Numerical modeling and design of inflatable structures – application to open-ocean-aquaculure cages. Aquacultural Engineering 33, 285-303. DOI: 10.1016/j.aquaeng.2005.03.001

Tsukrov, I., Drach, A., Decew, J., Swift, M.R., Celikkol, B., 2011. Characterization of geometry and normal drag coefficients of copper nets. Ocean Engineering 38, 1979-1988. DOI: 10.1016/j.oceaneng.2011.09.019

Tsukrov, I., Eroshkin, O., Fredriksson, D., Swift, M.R., Celikkol, B., 2003. Finite element modeling of net panels using a consistent net element. Ocean Engineering 30(2), 251-270. DOI: 10.1016/S0029-8018(02)00021-5

Xu, T.J., Zhao, Y.P., Dong, G.H., Bi, C.W., 2014. Fatigue analysis of mooring system for net cage under random loads. Aquacultural Engineering 58, 59-68. DOI: 10.1016/j.aquaeng.2013.10.004

Xu, T.J., Zhao, Y.P., Dong, G.H., Gui, F.K., 2013. Analysis of hydrodynamic behavior of a submersible net cage and mooring system in waves and current. Applied Ocean Research 42, 155-167. DOI: 10.1016/j.apor.2013.05.007